Bioinspiration & Biomimetics

OPEN ACCESS

RECEIVED
8 June 2020

REVISED
7 January 2021

ACCEPTED FOR PUBLICATION
4 February 2021

PUBLISHED
1 March 2021

PAPER

Wrist-driven passive grasping: interaction-based trajectory adaption with a compliant anthropomorphic hand

Kieran Gilday, Josie Hughes and Fumiya Iida*

Bio-Inspired Robotics Lab, Department of Engineering, University of Cambridge, United Kingdom
* Author to whom any correspondence should be addressed.

E-mail: kg398@cam.ac.uk, jaeh2@cam.ac.uk and fi224@cam.ac.uk

Keywords: anthropomorphic hand, compliant interactions, passive grasping, wrist control

Abstract

The structure of the human musculo-skeletal systems shows complex passive dynamic properties, critical for adaptive grasping and motions. Through wrist and arm actuation, these passive dynamic properties can be exploited to achieve nuanced and diverse environment interactions. We have developed a passive anthropomorphic robot hand that shows complex passive dynamics. We require arm/wrist control with the ability to exploit these. Due to the soft hand structures and high degrees of freedom during passive-object interactions, bespoke generation of wrist trajectories is challenging. We propose a new approach, which takes existing wrist trajectories and adapts them to changes in the environment, through analysis and classification of the interactions. By analysing the interactions between the passive hand and object, the required wrist motions to achieve them can be mapped back to control of the hand. This allows the creation of trajectories which are parameterized by object size or task. This approach shows up to 86% improvement in grasping success rate with a passive hand for object size changes up to ±50%.

1. Introduction

Trajectory generation for a complex, compliant hand–arm system is a significant challenge [1–3]. This is due to the interdependence between the trajectory of the arm, and the physical, passive interactions between the hand and the environment [4]. There has been the development of complex manipulators that show impressive in-hand manipulation skills [5], however, there are limited methods for generating trajectories which exploit these capabilities [6]. Conversely, we have seen the development of trajectory planners for 'single point' gripper such as pinch grippers, or the universal gripper [7–9]. However, the complexity of the physical interactions that can be achieved using these grippers is limited, restricting the behavioural diversity and adaptive grasping capabilities [10, 11].

To move towards more human-like, general-purpose grasping we need increasingly diverse and nuanced interactions between the environment, object and the hand [12]. To achieve this, we need to consider the design and interplay between the passive properties of the hand, and also the trajectory of the hand relative to the environment [13, 14]. Rather than generate bespoke trajectories on a case-by-case basis, our goal is to take existing trajectories which leverage passive interactions, and intelligently adapt these for changes in the environment.

Automated trajectory generation for all joints or degrees of freedom of a compliant hand–arm system is unfeasible. This is due to the number of unique joints, and range of environmental interactions that can occur [8, 15, 16]. Instead, we need higher-level approaches, which allow passivity and self-organization between the hand and the environment to be accounted for [17–19]. To achieve this, we need to understand the interplay between the physical adaption of the hand during interactions, and the trajectory of the hand during grasping [4]. This is outlined in figure 1, where the complex interactions depend on many factors including the wrist control, hand design and the object/environment. By understanding interactions, we can adapt existing trajectories to improve capabilities rather than generating bespoke trajectories.

The objective of this paper is to investigate a framework for generating wrist trajectories for human-like hands that utilize passive dynamics [20]. In this framework we consider actuating only the

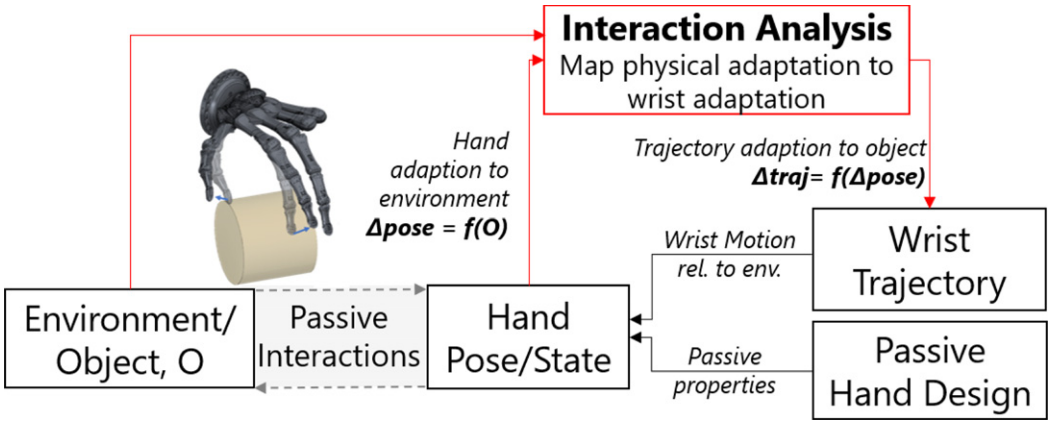

Figure 1. Outline of conceptual framework. Passive interactions between the hand–object–environment are dictated by the hand design as well as the wrist trajectory, by understanding these interactions, i.e. how the hands posture changes during specific interactions, the wrist trajectories can be modified to complete the same interactions robust to changes in the object/environment. Hence, adaptive grasping can be achieved without having to generate bespoke trajectories.

wrist of a passive hand, as to allow the passive interactions to be exploited. The central concept of this framework is 'interaction analysis' of demonstrated wrist grasping trajectories. By analysing the passive interactions that occur during a demonstrated grasping trajectory, we can identify how wrist motion triggers these interactions. Specifically, we can classify the different types of physical interactions between the hand and the object during grasping, and identify rules for adapting the wrist trajectory for different objects, where the rules aim to preserve the interactions for changing objects. In this way, we can perform trajectory adaptation based on passive interaction analysis, using an improved understanding of the role of hand adaptations to improve trajectory planning.

To demonstrate the importance of hand–environment interactions, we construct a human-like passive hand which shows passive-adaptive behaviours when performing human-like grasps. We then investigate the use of wrist control to achieve passive grasping in four case studies which each explore grasping of spheres using different interaction-based strategies. The 'interaction analysis' then enables us to process the demonstration trajectories into more general 'template' trajectories, which improves grasping robustness to changing object size and allows adaptation to grasp similar objects with size changes up to $\pm 50\%$. To show real world applicability, a range of everyday objects were grasped using this method, by approximating the objects of spheres and using the trajectory templates. The successful grasping of these objects demonstrates the versatility of the human-like passive hand and the 'interaction analysis' of wrist trajectories.

'Interaction analysis' allows us to better understand the role of passive interactions during grasping. This method provides wrist controllers for hands which have a physically complex embodiment. It enables the continued exploitation of interactions with inexpensive physical training/demonstration; only a single demonstration is required to complete a range of tasks. In addition, this approach can be applied to a wide range of compliant systems as it is independent of the specific hand design or dynamics.

The remainder of this paper is structured as follows: section 2 details the design and construction of the passive hand itself, as well as the architecture for wrist control and generation of trajectories. Section 3 contains the experimental setup, with detail of the robot platform and method for recording trajectories. Section 4 is the experimental results, showing the processing of demonstrations into templates and the results for parameterisation and adaptation of four grasp types. Finally, the conclusions and discussion are presented in section 5.

2. Methods and materials

Our system is comprised of two major components, the passive hand and the accompanying wrist controller based on 'interaction analysis'. The anthropomorphic design provides tune-able passive behaviours and enables highly nuanced environmental interactions to be achieved. The wrist controller processes demonstration trajectories into classifiable interaction states, which form 'template' trajectories, designed to exploit environmental interactions to grasp a wide range of objects.

2.1. Passive hand design

Figure 2 shows the passive hand design; many design choices reflect properties of the human hand. The hand consists of only the thumb, index and middle fingers as much of human grasping can be achieved with these three fingers; this can be seen in the GRASP taxonomy [21].

The bones of the hand have anthropomorphic proportions, positions and rolling contact

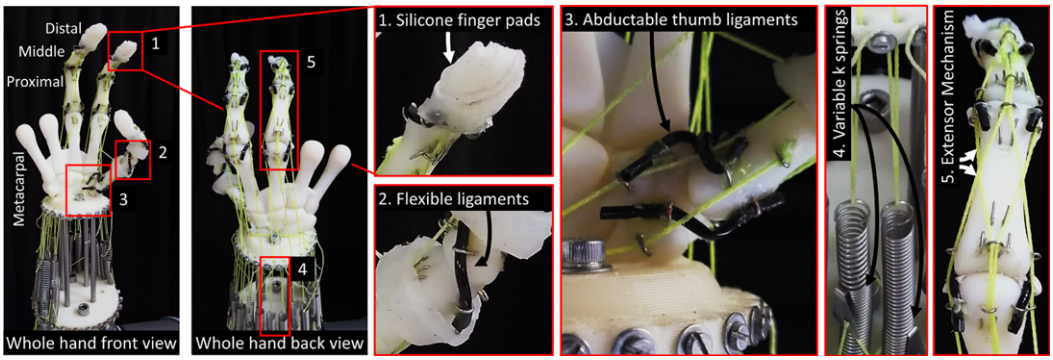

Figure 2. Passive hand design, front and back view, with highlights of critical design features. (1) Silicone finger pads to mimic human skin and increase friction. (2) Flexible ligaments limit unwanted motion and add passive stiffness. (3) Abductable thumb ligaments and bone shape approximate full thumb motion. (4) Variable stiffness springs, via constraining hooks, allow adjustment of starting pose and compliant hand behaviour. (5) Extensor mechanism with three tendons.

surfaces [12]. These bones are manufactured using a Stratasys Objet500 printer with standard rigid ABS material, RGD450, and are printed with many small holes for ligament anchors and tendon pulleys. There are deviations in the bone design between our passive hand and a human hand. The carpal (palm) and metacarpal bones of our design are fixed. Human hands have a small range of motion in the metacarpal bones, the most significant motion in the metacarpal of the little and ring finger, which are omitted from our design. Human carpal bones have complex motions facilitating wrist bending, which is achieved in this work using a 6DoF robotic arm.

Each phalanx (proximal, middle and distal) is effectively floating. One finger bone is connected to the next with the joint motion restricted to a useful range by using a combination of bone joint geometries, tendons and ligaments. If only tendons were used, each joint can twist and slip in unpredictable ways. Conversely, if only ligaments were used, there would be no compressive force keeping the joints in contact. As each joint is formed with these compliant elements, the fingers themselves can comply when interacting with the environment, but are still effectively controlled in the actuated degrees of freedom by the tendons. Therefore, stiffness can be adjusted in the major axes through tendon tension.

The contact surface geometry of the bones plays a significant part in determining the compliance of each joint axis [22]. One particular example which demonstrates this is the difference between the proximal-metacarpal joint and the proximal-middle/middle-distal joints. The proximal-middle joint can be approximated by the rolling interaction of two cylinders; therefore compliance outside of the flexion/extension axis is limited. However, the proximal-metacarpal joint differs in that the metacarpal bone has a more ellipsoidal shape, increasing compliance in the abduction/adduction axis [23, 24].

The ligaments are made from flexible 2 mm tubing and form an ‘S’ shape over the majority of joints, connecting to the anchor points on the palmar side of the distal bones and the back of the proximal bones. This type of ligament allows the bones to roll but not slip [25], and ensures the bones return to the same positions. Additionally, the ligaments introduce passive stiffness to each joint and limit lateral motion and longitudinal rotation [26].

The thumb metacarpal-carpal joint differs in design to the others, the bone shapes more closely resemble two interlocking saddles and three ligaments connect the bones together. A pair of ligaments form an ‘X’ over the thumb and index metacarpal bones and the third prevents slip when fully extended and adducted. This geometry and ligament configuration allows much greater range in the abduction/adduction axis with respect to the other joints [20].

The tendons are constructed from Hercules PE Braided Line. Each tendon is connected to an adjustable spring to allow for control of tension and stiffness. Figure 2(4) shows the mechanism for adjusting stiffness; here, the hooks can be used to constrain a portion of the string to prevent it from extending, changing the stiffness by altering the effective length of the spring. The tendon length can be shortened or lengthened for control of tension. The combination of tendon properties defines the hands passive behaviours.

The starting posture is defined by the equilibrium between the tendons in each finger. Each finger has four degrees of freedom, full actuation can be achieved with correct routing of five tendons [27]. The index and middle finger have two flexor tendons, one connected to the distal phalanx and one to the middle phalanx. Three tendons form the extensor mechanism, one tendon connects to the distal phalanx then splits and runs on each side of the proximal-middle joint before joining into a single tendon. The final two extensor tendons connect to the

Figure 3. Passive hand fabrication process. (a) 3D printed bones, cleaned and organised, (b) metal pins for tendon and ligament anchor points epoxied in place, (c)and(d) ligaments attached at both ends, (e) tendons attached and routed to adjustable springs.

middle phalanx and split to run either side of the metacarpal-proximal joint. This tendon distribution approximates human anatomy and previous robotic finger designs [28].

Silicone fingertips are glued to the distal and thumb phalanges to increase the friction for grasping. A full skin can be cast directly onto the hand, although this prevents maintenance and modification, so only the area's most commonly used for grasping are covered.

The fabrication process of the hand can be seen in figure 3. The bones are printed and cleaned; the anchor and pulley holes are flushed of support material. Steel anchor and pulley pins are glued in place with epoxy. The ligaments are attached in two stages with epoxy, first to the proximal bones then the distal. Finally, the ligaments are trimmed, and the tendons are routed and attached to springs.

2.2. Interaction-based wrist control

Compared to an actuated hand, a passive hand requires more complex wrist control, even for simple grasping tasks. For successful grasping, the fingers must be stretched open first in order to provide a holding force or to cage the object for form closure. This requires careful interactions with the environment and object. Figure 4 outlines this passive interaction-based grasping concept for an object in a known location relative to the hand.

Figure 5 shows the interaction analysis framework for generating template trajectories from an input demonstration trajectory, then the adaptation and application to similar tasks with geometrical changes in the object/environment. The input to the trajectory processor is a series of robot poses and the object parameters. First, the trajectory is simplified and denoised by reducing down to a much smaller set of 'key states'. These key states are obtained by observing changes in behaviour during the grasp and are seen as inflection points in the trajectory time-series. These key states form the reference trajectory **R**, which is generated by interpolating between these points. Next, the states are classified by observing the interactions between the hand and environment. This is currently achieved manually, although has potential to be automated with proprioception [18] or external cameras. Each class has an update policy for adaptation to changing object geometry, which takes the object parameters **L** and interaction information (contact planes between the hand and object) between the fingers and environment resulting in a transformation of $\Delta(\mathbf{L})$. The template trajectory **T** is given by the reference **R** plus this transformation.

2.3. Contact-oriented key states

The robot steps through multiple behaviours to achieve stable passive grasping. These behaviours are classified, and an update policy for each type of interaction can be defined. The update policy is designed to preserve interactions and prevent unwanted interactions.

The classification of the interaction types can be seen in figure 6. There are three types depending on how many points of contact have induced interactions

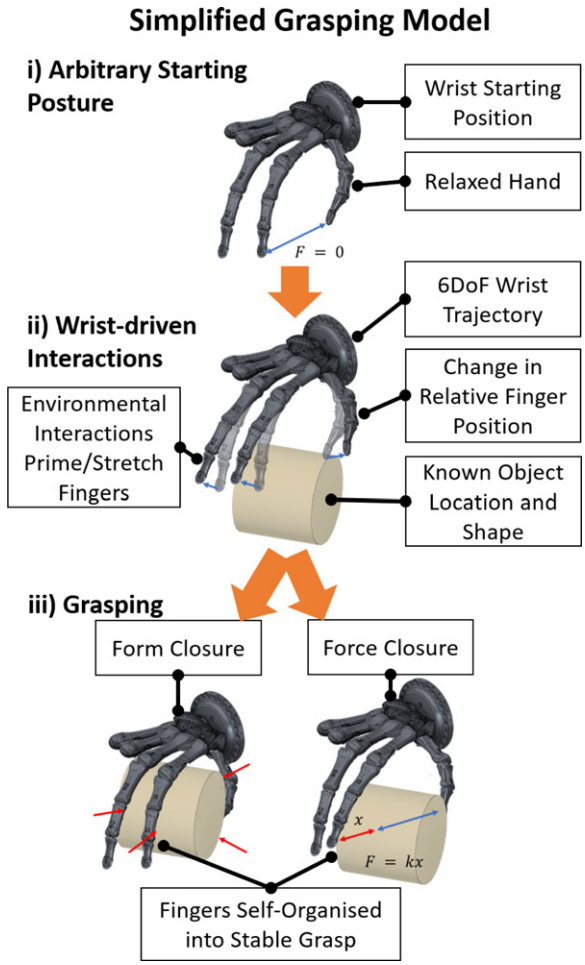

Figure 4. Grasping model. To successfully grasp (either form or force closure) first the fingers must be stretched open through interactions with the object and environment, either to insert the object inside a cage or between two or more fingers now exerting force from internal springs.

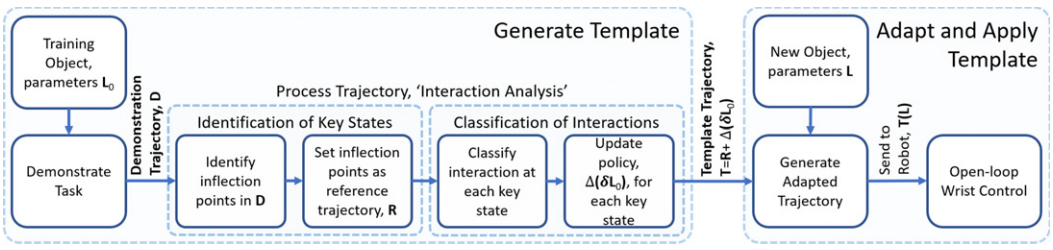

Figure 5. Flowchart of passive grasping based on the adaptation of 'template' trajectories rather than generation of bespoke trajectories. An input demonstration trajectory on a basic object with parameters L_0 is processed by analysing the interactions, to generate a template trajectory, **T**. The template can then be adapted to a new object by inputting the change in parameters compared to the training object. The adapted trajectory is then performed by the robot.

when the robot transitions to that state, zero, one, or more than one, i.e. no contact, single contact and multiple contact states:

- *No contact*: these are transition states when the hand and object have no contact, or when wrist motions induce no interaction. The update policy for this is a parameterised translation to prevent unwanted interactions that could occur from change in the object size.
- *Single contact*: when wrist motion induces an interaction through a single contact plane. For example, when pressing two fingers onto the top of an object. To parameterise, the position of the object relative to the non-interacting fingers is preserved, therefore a translation, normal to the plane of contact and proportional to the change in objects geometry, is added.
- *Multiple contact*: when wrist motion induces interaction through multiple contacts which are not independent. For example, when the object

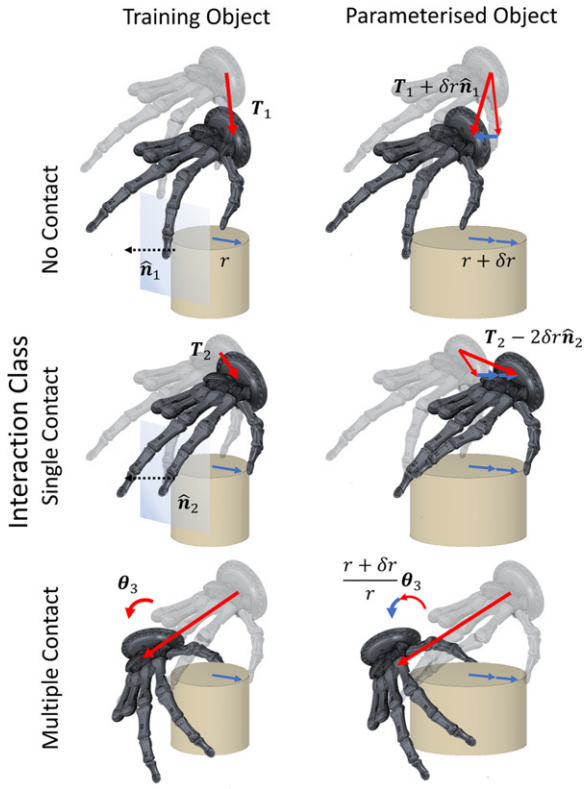

Figure 6. Classifications of key states. Example interactions and how they are adjusted by the change in radius of a cylinder. No contact class: the finger follows the change in surface so there is no change in interaction. Single contact: finger remains in contact, interaction is increased to preserve objects position relative to the rest of the hand. Multi contact: orientation is adjusted to increase or decrease the distance between interacting fingers, in order to keep the finger strain approximately constant over changing object parameters.

is inside the hand and the contact of multiple fingers on opposing object faces must be preserved. This requires a change in orientation, in addition to a shift, to narrow or widen the distance between fingers proportionally with the change in objects geometry.

A key state can have multiple of these types of interactions if each separate interaction can be extracted independent of the others, i.e. if the contact planes are orthogonal.

The input trajectory **D** is described by a time series of robot poses:

$$\mathbf{D}_i = [x_i, y_i, z_i, rx_i, ry_i, rz_i]_{i=0,\,\ldots n-1} \tag{1}$$

Where the pose is the combination of Cartesian position x, y, z and axis-angle rotation rx, ry, rz, with n poses in the trajectory and the poses are sampled at 10 Hz using the UR5 arm internal position data.

Interpolating between k carefully selected key states, **R**, retains sufficient subtly for successful grasping

$$\mathbf{R}_i = [x_i, y_i, z_i, rx_i, ry_i, rz_i]_{i=0,\,\ldots k-1}. \tag{2}$$

Each state will also have a set of finger contacts and contact orientation. This data describes how the states are parameterised into the template trajectory **T**:

$$\mathbf{T}_i = \mathbf{R}_i + \Delta_i$$

$$\mathbf{T}_i = [x_i, y_i, z_i, rx_i, ry_i, rz_i] + [\delta x_i, \delta y_i, \delta z_i, \delta rx_i, \delta ry_i, \delta rz_i] \tag{3}$$

where the Δ vector shifts and rotates the trajectory depending on the state classification. A *no contact* state translates away from the contact plane, defined by the normal $\underline{n}$, by the scalar change in object geometry δl:

$$\Delta^{\mathrm{nc}} = \left[\delta l.\underline{n}^{\mathrm{T}}, 0, 0, 0\right]. \tag{4}$$

A *single contact* state is translated similarly, but in the opposite direction, so a larger object will induce more deformation in the hand:

$$\Delta^{\mathrm{sc}} = \left[-\delta l.\underline{n}^{\mathrm{T}}, 0, 0, 0\right]. \tag{5}$$

A state may require multiple shifts due to multiple independent single contacts, in this case the component in each axis is calculated, with the final translation is given by the mean of these components.

The Δ for a *multiple contact* state contains a rotation component, in addition to shifts. The rotation component is an interpolation or extrapolation of the rotation vector between that state and the previous:

$$\Delta^{\mathrm{mc}} = \left[-\delta l.\underline{n}^{\mathrm{T}},\ F(\boldsymbol{\theta}_{-1}, (1 + \frac{\delta l_r}{l_r})F^{-1}(\boldsymbol{\theta}, \boldsymbol{\theta}_{-1})) - \boldsymbol{\theta}\right] \tag{6}$$

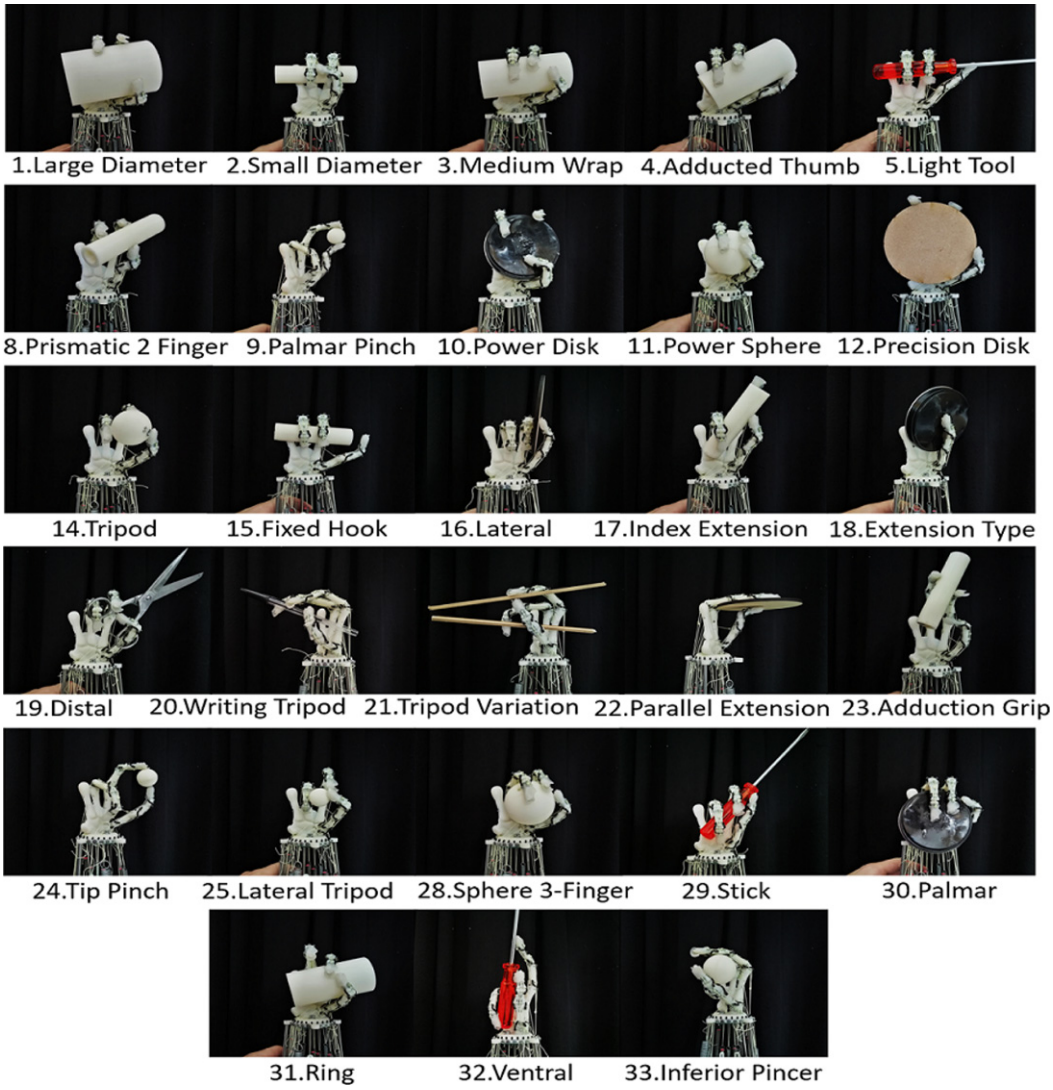

Figure 7. The passive hand performing 28 of the 33 grasp types from the GRASP taxonomy [21], with manual adjustment of starting posture.

where $\boldsymbol{\theta}$ is the current states axis-angle orientation vector and $\boldsymbol{\theta}_{-1}$ is the previous states. F^{-1} subtracts axis-angles to get the change in rotation and F sums to give the new orientation vector.

This set of update rules allows fast application of the template trajectories to new objects by simply inputting the change in geometry, such as the diameter of a sphere. If these rules generalise to multiple objects and grasp types, then automation just becomes a problem of key state extraction and classification.

The advantage of classifying in terms of the interactions is that it removes any dependency on the hand design. The translations and rotations make no assumption of the hand design other than that the interaction can be completed. Therefore, this 'interaction analysis' can be easily applied to other hands.

2.4. Achievable grasp types

With no constraint on starting posture, the passive hand is able to perform 28 of the 33 grasp types from the GRASP Taxonomy [21], as seen in figure 7. This shows our hand design offers human-like range of motion. The remaining five grasp types all require a full five-fingered hand. Some of the achievable types are limited in terms of object holding force, mainly the adduction grip (23), the prismatic grip (8) and the pinches (9 and 24) as these all rely on force closure rather than form closure.

When constrained to a single starting posture, the set of achievable grasp types is more limited. Despite this, there exist starting postures with highly adaptive capabilities.

This paper focuses on a single type of object and the grasp types applicable with a single starting posture. It was found during manual exploration that the grasp types: adducted thumb, lateral tripod, sphere three-fingers and ring grasp where all achievable from a single starting hand posture. These are the focus of experiments in the following sections.

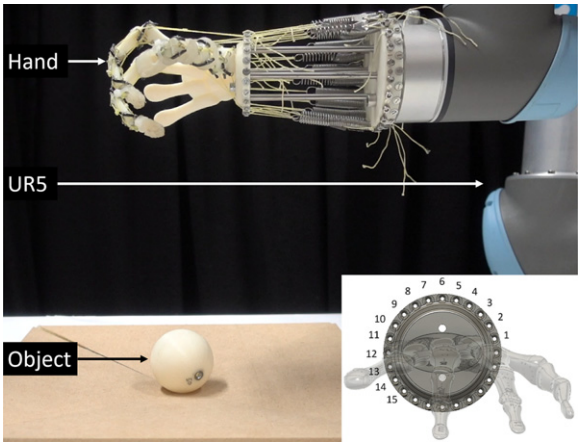

Figure 8. Experimental setup. Passive hand mounted on UR5 robot arm. Object is placed into a gentle depression to keep object position constant. Inset: top down hand, starting posture is defined by the tension and stiffness of each tendon 1–15.

Table 1. Tendon tension and stiffness for the starting posture in figure 8 and all experiments. Tendons are named: finger—action—connected phalanx, and correspond to the positions in figure 8 inset.

Tendon	Finger	Function	Anchor	T_0/N	k/N m^{-1}
1	Index	Flexor	Distal	4.3	0.31
2	Index	Flexor	Middle	1.8	0.27
3	Index	Extensor	Left	1.6	0.11
4	Index	Extensor	Distal	5.0	0.27
5	Index	Extensor	Right	2.0	0.10
6	Middle	Flexor	Middle	2.1	0.25
7	Middle	Extensor	Left	1.8	0.10
8	Middle	Extensor	Distal	3.9	0.25
9	Middle	Extensor	Right	1.8	0.10
10	Middle	Flexor	Distal	4.2	0.22
11	Thumb	Extensor	Distal	1.3	0.09
12	Thumb	Extensor	Middle	1.4	0.09
13	Thumb	Adductor	Proximal	1.3	0.10
14	Thumb	Flexor	Distal	7.6	0.68
15	Thumb	Abductor	Proximal	4.0	0.22

3. Experimental setup

Figure 8 shows the setup for recording and executing trajectories, with the passive hand mounted on a UR5 arm. For demonstrations, the arm is set to free-drive, a human guides the hand to grasp an object which is placed in a shallow depression so the position remains constant between trials. The absolute position and orientation of the centre of the palm is sampled at 10 Hz. The inset shows the top-down view of the hand and tendons which correspond to table 1.

The starting posture, seen in figure 8, is defined by the equilibrium of the tendon tensions and stiffness seen in table 1. The force due to gravity on the fingers is negligible relative to the tendon forces; there are minor variations in starting posture from hysteresis, originating from tendon friction.

The posture is kept constant for all experiments. This posture has moderately curled fingers and the thumb partially abducted, the exact starting joint angles are meaningless except in the context of the specific template trajectories trained later. This was chosen as it appears natural, and the fingers are positioned such that many different form and force closures can be achieved by selecting combinations of contact points. The stiffness of each joint has a non-linear relationship with the contributing tendons due the dislocate-able rolling joint and frictional components. When combined with the tendon arrangement over each joint, allows fine anisotropic control of compliance [12, 27]. As seen in table 1, the flexor tendons are generally set to higher stiffness. This provides large restoring forces when the fingers are extended (when the hand is opened), therefore large objects can experience greater holding forces.

3.1. Experimental method

Once the posture of the hand has been set, the grasp types for a sphere of diameter 50 mm are explored, this includes: sphere three-fingers, ring, lateral tripod and adducted thumb [21]. A human operator guides the robot and tries various grasping methods, successful grasps are recorded as demonstrations, only a single successful demonstration is required for each

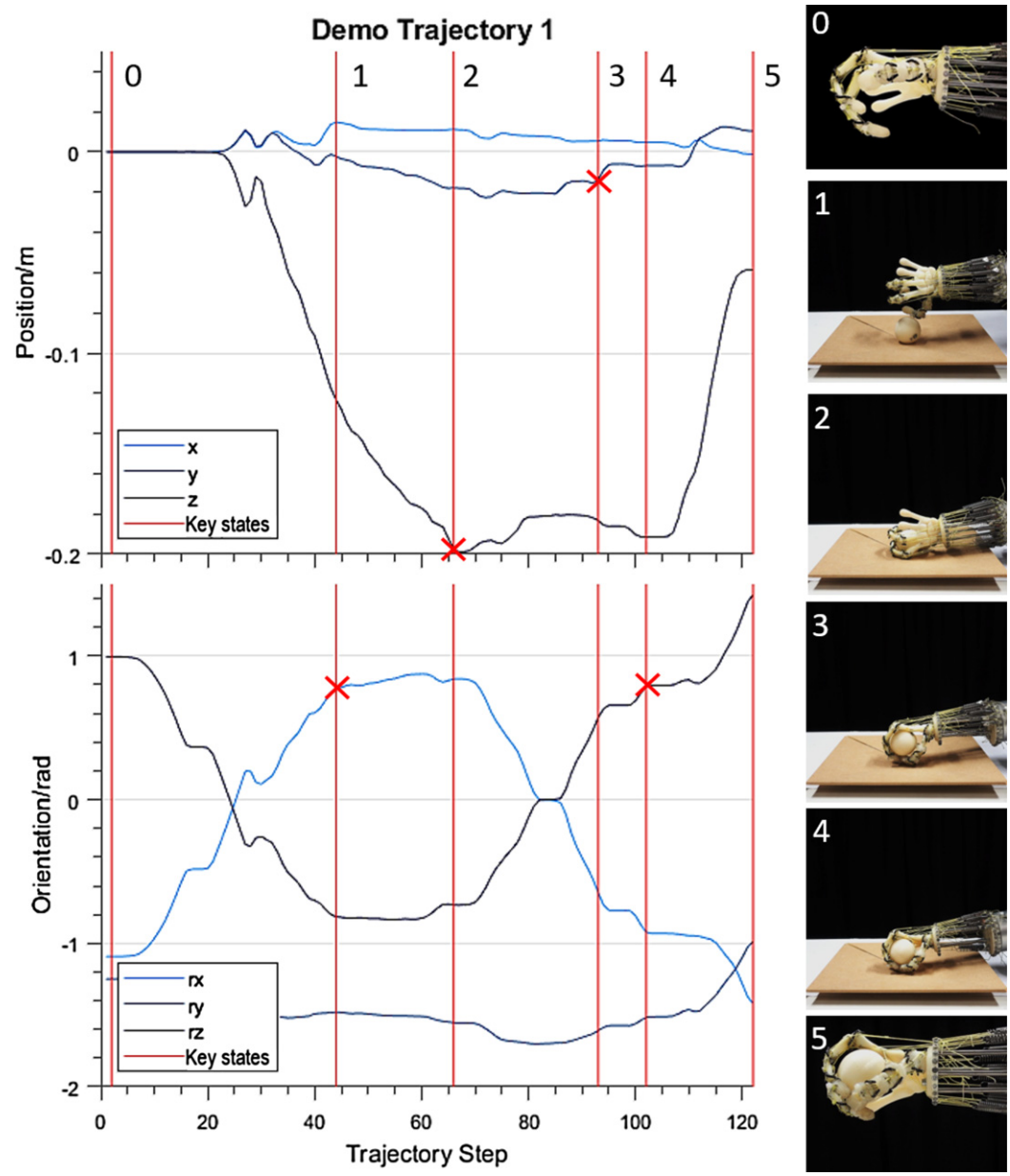

Figure 9. Demonstration trajectory for a 'sphere three-fingers' grasp type (blue), key states (red) mark the behavioural transitions and match to inflection points in position and/or orientation. The most critical axis for deciding each key state is marked with an 'X'. Images corresponding to the trajectory key states are shown.

grasp type. Once the demonstration is recorded, the template is generated through the process outlined in figure 5. These are then evaluated, in terms of their success rates when grasping spheres of changing size using the same robot setup. The sphere is placed in a known location and the hands posture is reset, the robot then performs the desired trajectory and the success or failure is recorded. This is repeated on spheres of varying size using both the template trajectory with no adaptation and the adapted template trajectory. This allows performance evaluation of the interaction-based trajectory adaptation.

Figure 9 shows the demonstrated trajectory of the 'sphere three-finger' grasp type for a sphere of diameter 50 mm. The key states are extracted by inflection points in the trajectories, these mark changes in behaviour. The states are classified manually by observing the interactions, these are: the starting state, re-positioning above the object (nc-no contact), pushing down onto the object (sc-single contact), re-positioning the middle finger to contact the ground (nc), pressing down to close the middle finger around the object (sc), finally the hand lifts and the object is grasped.

Figure 10 shows the same key state extraction for the 'ring' grasp type. Both of these trajectories clearly show the transitions between different behaviours at the inflection points, the point most significantly affecting the decision to extract as a key state are marked.

The demonstration procedure, as well as the achievable grasp types and example adaptations can

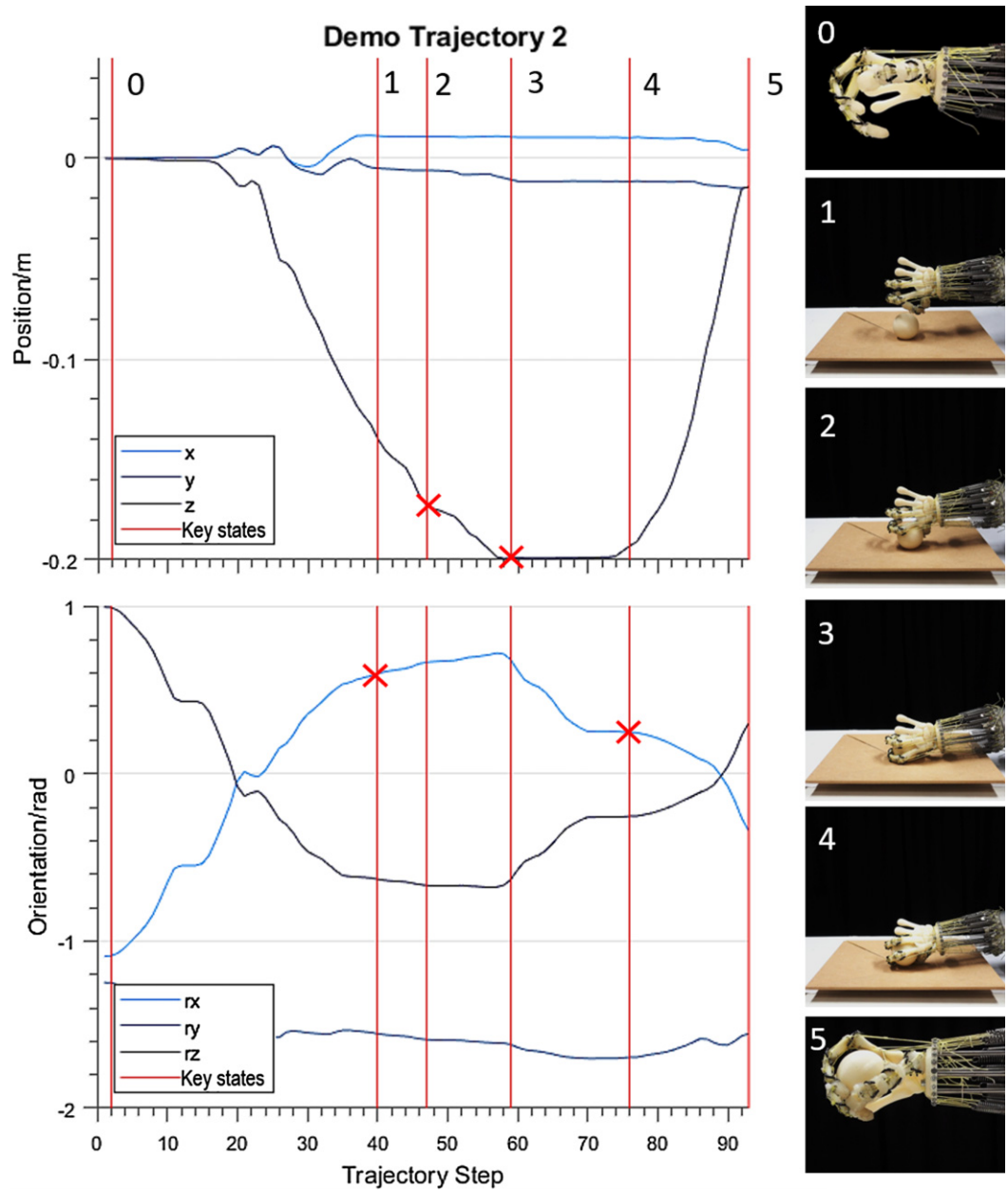

Figure 10. Demonstration trajectory for a 'ring' grasp type (solid blue), key states (red) mark the behavioural transitions and clearly match to inflection points in either the position or orientation. The most critical axis for deciding each key state is marked with an 'X'. Images corresponding to the trajectory key states are shown.

be seen in the accompanying video[1].

4. Experimental results

Figure 11 shows the subset of achievable grasp types for a single starting posture and a sphere of 50 mm diameter, and the set of key states required to achieve each grasp. Each distinct grasp type transitions through a unique set of key states.

The 'sphere three-fingers' grasp is characterised by the secure grasp using the inside of every finger. The ring grasp primarily uses just the inside of the index and thumb, where the thumb is abducted to form a ring around the object. The lateral tripod has a slightly adducted thumb and presses the object into the side of the middle finger with support from the index. Finally, the adducted thumb grasp shows much greater adduction and the object is supported by the thumb, the palm and the side of the index finger. Each grasp type has strengths and weaknesses in terms of speed and reliability, additionally, some grasp types more readily adapt to positive or negative changes in geometry using the basic update rules defined earlier.

4.1. Parameterisation

Figure 12 shows the template trajectories of the four grasp types from figure 11. The adapted trajectories (solid area) at each key state shows the Δ,

[1] Link to accompanying video: https://tinyurl.com/passive-hand.

which is proportional to the change in the object's parameter. For a sphere, there is only one parameter, the diameter. Much of the adaptation comes from translations, only the ring and adducted thumb grasps have significant changes in orientation.

The sphere three-finger trajectory, figure 12(a), is formed from six key states, the Δ for each state due to a radius change of δr is given by:

$$\Delta_0 = [0, 0, 0, 0, 0, 0]$$
$$\Delta_1 = [0, 0, 2\delta r, 0, 0, 0]$$
$$\Delta_2 = [0, -2\delta r \sin\frac{\pi}{4}, 2\delta r \cos\frac{\pi}{4}, 0, 0, 0]$$
$$\Delta_3 = [0, 0, 2\delta r, 0, 0, 0]$$
$$\Delta_4 = [0, 2\delta r \cos\frac{\pi}{3}, 2\delta r \sin\frac{\pi}{3}, 0, 0, 0]$$
$$\Delta_5 = [0, 0, 0, 0, 0, 0]$$

Where the starting state, 0, is transformed by Δ_0, the remaining transformations apply to the key states seen sequentially in figure 11. This grasp type ends with the sphere securely enclosed between all three fingers. The grasp is carried out by pressing the sphere between the index finger and thumb, then re-orienting and pressing the middle finger into the sphere, for additional support, using the ground.

The first non-starting state, 1, is a no contact state where the thumb and index finger should remain above the object, therefore a z-shift proportional to the change in the object's height is added. Key state 2 is a single contact state, comprising of three independent interactions. First, the index finger is in contact in a plane on the underside of the sphere pointing down and away from the camera, this introduces a shift upwards and towards the camera. Second and third, the palm and middle finger both are in no contact states, the palm introduces a shift towards the camera by the radius change, the middle finger is positioned midway up the sphere, so introduces a positive z-shift by the radius change. The geometric mean of these is a shift of twice the radius in the vector pointing up and towards the camera.

The third state is a no contact state, where the sphere is now roughly held in the hand, but the underside remains at the same height relative to the ground, therefore is shifted upwards by twice the radius change. The fourth state pushes the middle finger into the ground following the contact plane between the middle finger and the ground, this plane points down and towards the camera at an approximately 60° angle to the vertical, resulting in a shift of twice the radius up and away from the camera.

The adducted thumb grasp, figure 12(d), has the following Δ for its five key states:

$$\Delta_0 = [0, 0, 0, 0, 0, 0]$$
$$\Delta_1 = [0, 0, 2\delta r, 0, 0, 0]$$
$$\Delta_2 = [0, 0, 2\delta r, 0, 0, 0]$$
$$\Delta_3 = [0, 0, \delta r, 2.31\delta r, 6.4\delta r, 5.79\delta r]$$
$$\Delta_4 = [0, 0, 0, 0, 0, 0].$$

The first non-starting state, 1, is a no contact state, positioning the fingers just above the sphere, so the sphere is positioned centrally between the thumb and index finger. Therefore, the contact plane is the top of the sphere, resulting in a shift upwards by the change in radius. Key state 2 is another no contact state, here the hand is pressed onto the sphere, until the palm is in contact, this has the same Δ as the previous state. State 3 is a multiple contact state, here the sphere is pressed into the ground, such that the thumb is forced outwards and the sphere is pinched between the side of the index finger and the thumb. This interaction takes place in the mid-plane of the sphere, pointing up, resulting in a shift by the change in radius to remain at the same height relative to the sphere. Additionally, a rotation component is added. The Δ_3 rotation in reality is a more complex function but approximated here for clarity. This increases the change in rotation when the sphere decreases in size, which increases the interactions between the hand, object and environment, resulting in a more secure grasp. Without this, the sphere is not positioned correctly inside the hand and insufficient holding force is provided for grasping.

4.2. Adaptive grasping

The wrist controller can now be evaluated on objects of varying size. To measure the success of the adapted trajectories, the adapted trajectories are compared to the non-adapted template trajectories (i.e. $\Delta = 0$) on spheres of changing diameter. In total, 11 sphere sizes are tested in diameter steps of 5 mm. Each sphere is tested 10 times for both the adapted and non-adapted trajectories and the success of each grasp recorded.

The variability in grasping success originates from slight changes in the hands starting posture and the objects relative position. Failures generally occur due to one of two reasons. Either the object collides with the hand in an undesired way, which results in the object moving relative to the hand or the robots protective stop activating. Alternatively, the interactions do not result in a great enough force to securely grasp, here the object tends to get dropped when lifting at the end of the trajectory.

Examples of failures and successful adaptations for the sphere three-finger grasp are shown in figure 13. Figure 13(a) shows the non-adapted trajectory failing to grasp to a sphere with 50% increase in radius compared the demonstration

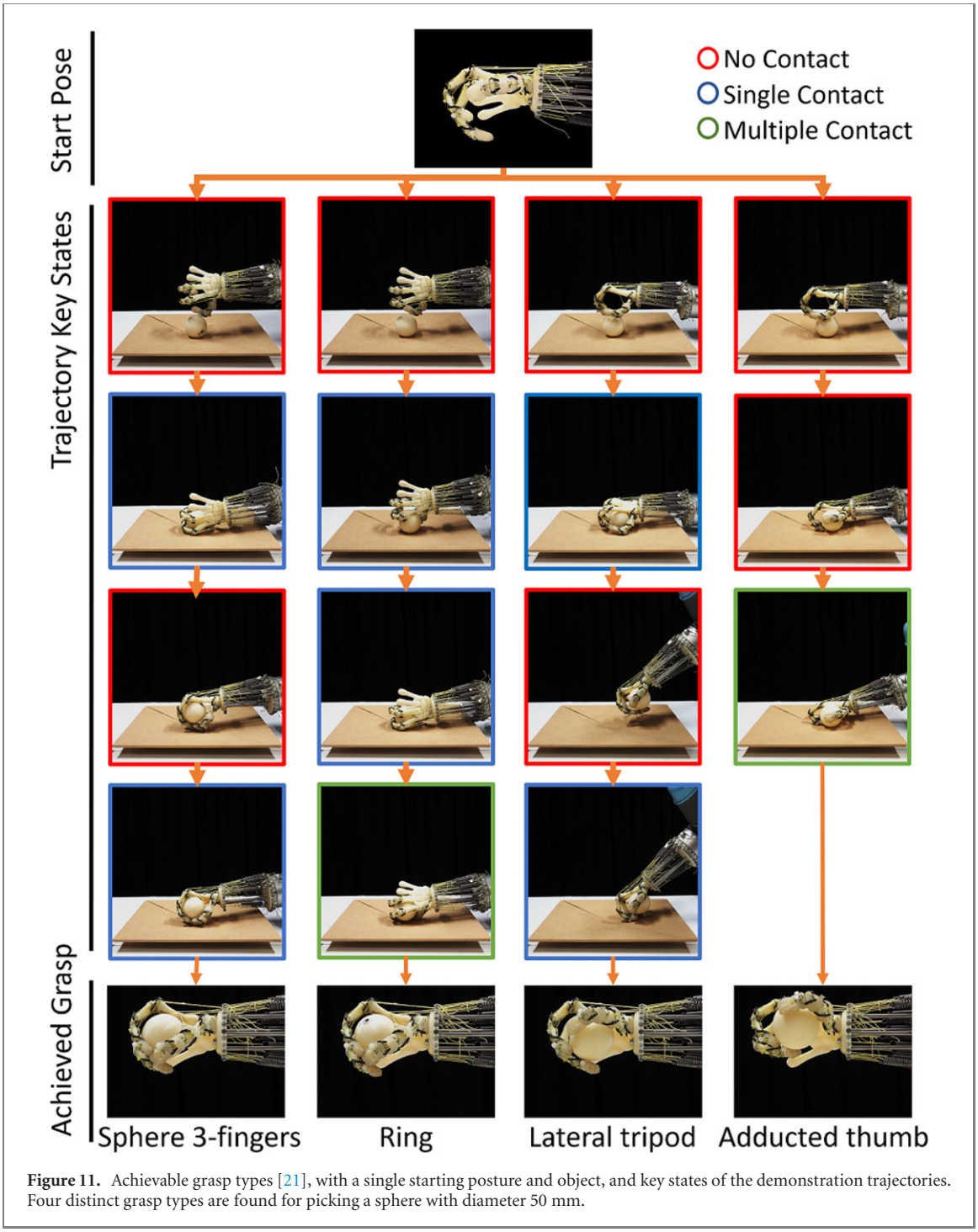

Figure 11. Achievable grasp types [21], with a single starting posture and object, and key states of the demonstration trajectories. Four distinct grasp types are found for picking a sphere with diameter 50 mm.

object. Figure 13(b) shows the trajectory successfully adapted to the same sphere. As the sphere is larger, with no adaptation, the first interaction happens unintentionally in the no contact state, shown in the top image: the sphere pressing into the thumb, rather than between the thumb and index. The second and third image show the resulting thumb deformation where the sphere is never enclosed in the hand. The adapted trajectory is able to position the thumb correctly in the first state, therefore state 2 successfully presses the sphere between the thumb and index finger. This allows continuation into the remaining states: adjustment in the third and fourth state prevent collisions with the ground, the final state shows the object successfully lifted.

Figure 13(c) shows the non-adapted trajectory failing to grasp a sphere with 50% reduction in radius, whereas figure 13(d) shows the successful adaptation. In the second state of figure 13(c), the hand is too high above the object and ground, this very loosely presses the thumb into the object, therefore insufficient holding force is provided and the next state fails as the object is released. The adapted trajectory presses much further downwards, the thumb is

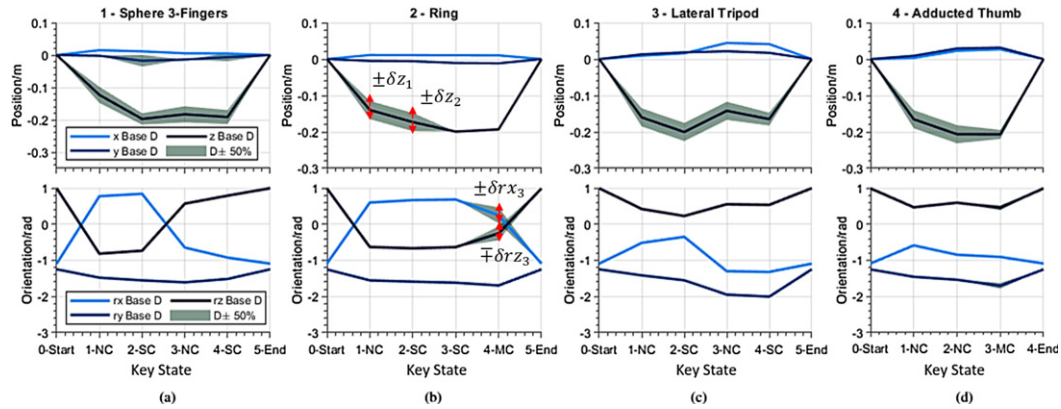

Figure 12. Template trajectories for the grasp types in figure 11. 6-dof trajectories: position (x, y, z) shown top, orientation (rx, ry, rz) shown bottom. Adapted trajectories (filled area) up to $\pm 50\%$ change in sphere diameter, depend on key state types and contact planes.

pressed into the ground and deformed towards the sphere, therefore some closure is provided and the next state is successfully carried out. Without adaptation, the fourth state would not result in contact the ground, reducing the chance of successful grasp as the middle finger is not re-positioned correctly for stabilising the grasp. The final image in figure 13(d) shows the smallest sphere successfully lifted.

Figure 14 shows the grasping success rates for all four grasp types, for both the adapted and non-adapted wrist trajectories. The non-adapted trajectories show the baseline capabilities of this compliant hand. The adapted trajectories show the improvements when augmenting with interaction-based wrist control. The hand is able to adapt and grasp spheres with changing size $\pm 50\%$.

The sphere three-finger, figure 14(a), shows good passive adaption without any alteration in wrist control for ± 10 mm diameter. For larger changes, the adapted trajectories show significant improvement, especially for the larger spheres.

The ring grasp, figure 14(b), only shows minor improvements at the extremes, similar to sphere three-finger. The lateral tripod grasp is more difficult to generalize, as seen by the poor success rate for the non-adapted trajectory. This trajectory is very sensitive to the finger and objects position, especially leaving key state 2 as the object is held very loosely, then lifted and pressed into the ground to secure the grasp. The performance with the adapted trajectory is far better, exceeding 80% for some sizes with 0% in the non-adapted case. Finally, the adducted thumb shows similar performance with adapted and non-adapted for smaller spheres, though the adapted trajectory has much superior performance for the larger spheres.

All grasp types have generally poor performance with the extremely small spheres. This can be solved by training new template trajectories based off grasping between smaller gaps between fingers, such as the adduction grip (figure 7(23)), or by adjusting the hands starting posture to favour smaller objects and training new template trajectories accordingly. Theoretically there is no minimum size object that can be grasped by starting the hand in an index-thumb pinch (figure 7(24)), though practically there are limits such as from the curvature of the fingertips.

The larger spheres tended to perform better as, if closure is achieved, there is almost always significant holding force due to large deformations in the hand. However, the larger spheres are also more likely to lead to unwanted collisions, either knocking the object away, or triggering protective stops in the robot due to excessive forces. Both of these result in grasping failure.

In each of the four grasp types, the adapted trajectories performed at least better at one or both of the sphere diameter extremes. The smallest improvements are seen in the cases where the hand already shows good adaptability. Considering the full range of spheres tested, the average success rate for the non-adapted trajectories is 34.8%, the adapted trajectories have 57.7%, a 66% increase. Excluding the results for the 50 mm sphere where the trajectories are identical, the average success rates become: 54.5% for the adapted, an 86% increase over the non-adapted at 29.3%. The average range of sphere sizes with at least one successful grasp for the non-adapted is 23.75 mm and for the adapted 45 mm, this is an 89.5% increase. Out of the 40 cases (four grasp types, 10 spheres excluding 50 mm), 27 showed an increase in grasping success rate, with the remainder being the same success rate or a small decrease within expected variability.

Figure 15 shows these four grasping strategies applied to a range of everyday objects. To apply a trained grasp type to a new object, the object should be approximated as one of the training objects. The template for the closest matching training object is chosen. In this case, there is only a single training object and the templates have been chosen such that they have a high chance of success on the geometry

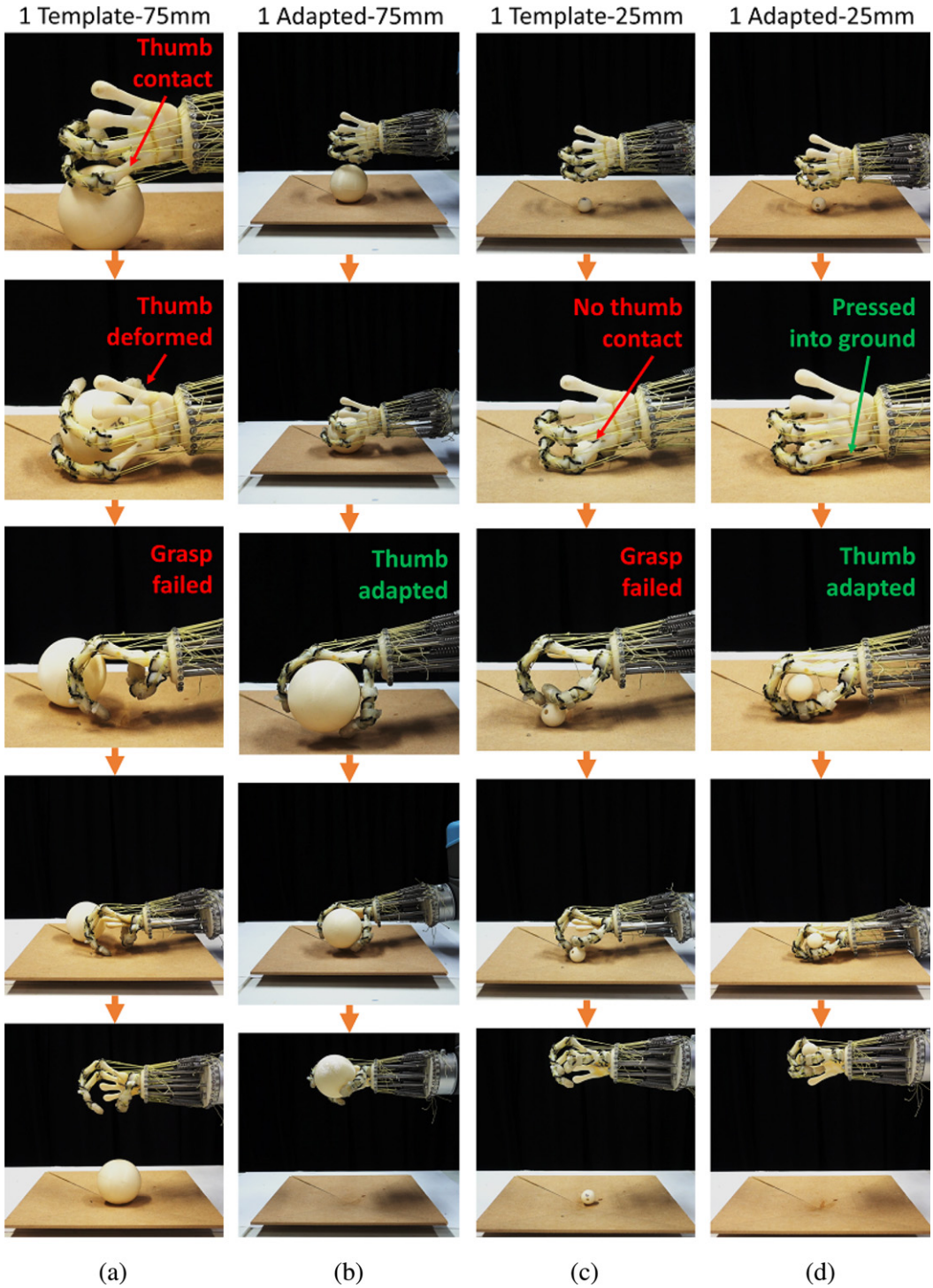

Figure 13. Failure mechanisms for 'sphere three-fingers'. The adapted trajectories for 75 mm and 25 mm sphere are compared to the non-adapted template trajectory. For the non-adapted 75 mm (a), the initial no contact state generates unwanted interactions when not adapted, causing the thumb to greatly deform so no closure is achieved for the non-adapted 25 mm (c), the distance between the thumb and index is too great so too little holding force is provided, whereas the adapted trajectory (d) is able to close the gap.

change of the object, e.g. sphere three-fingers and lateral tripod are better at adapting to smaller objects (figure 14). Due to the complex design and passive dynamics of the hand, grasping can still be achieved with high variations in object shape, though the success rate will generally be lower than for a perfect sphere of the same size. These everyday objects have different weights and frictional properties than the training object. The grasping success shows the versatility of our approach. However, if these differ too much the grasp is more likely to fail and new template trajectories should be trained.

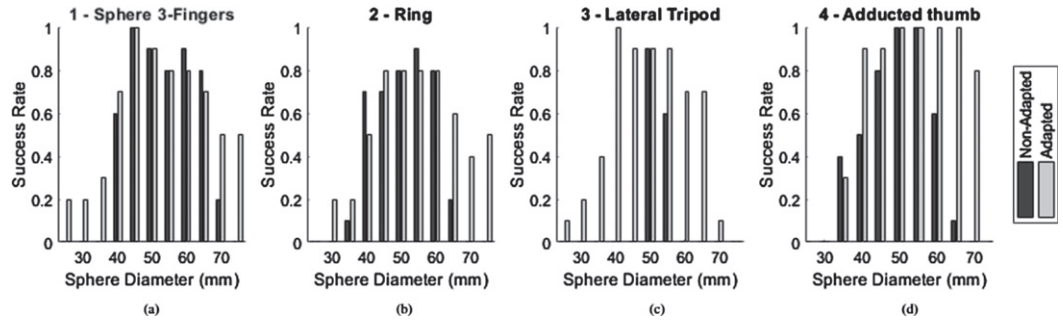

Figure 14. Grasping success rates of trajectories for four grasp types. Non-adapted trajectory, $\Delta = 0$ (dashed line), compared with the adapted trajectories for 11 spheres ranging from $D = 25$ mm to $D = 75$ mm (solid line). At $D = 50$ mm the trajectories are identical.

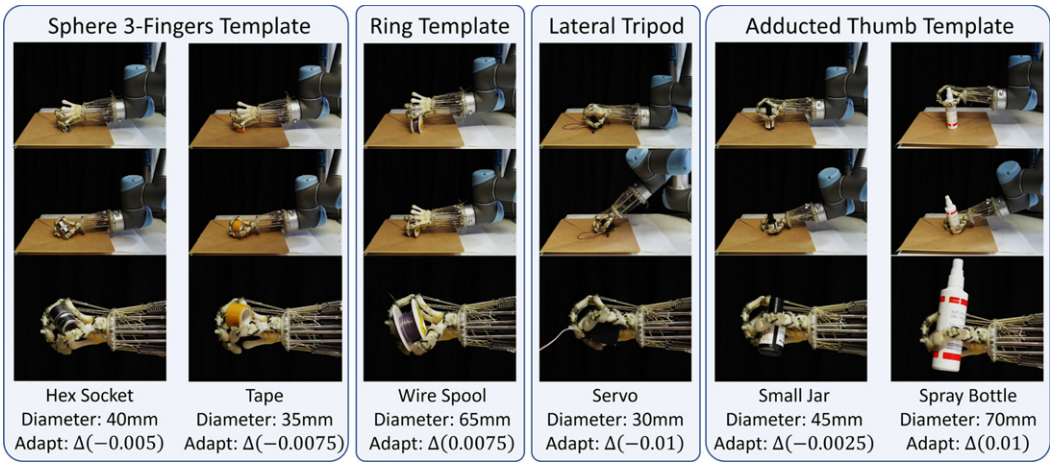

Figure 15. Trained grasping strategies applied to a selection of everyday objects approximated to spheres with the listed diameters.

5. Conclusions and discussion

Compliance and passive dynamics are increasingly being used in robotic hands [10], with imitation of biological structures providing a common way of incorporating these elements [29]. To make use of such robotic hands, new trajectory generation approaches are required that exploit the passive elements. By considering the mapping between the physical interactions between the hand–object–environment and wrist position, we provide a method for adapting wrist trajectories for generalized grasping, rather than the less practical approach of generating bespoke trajectories for each new object. Central to this, is the concept of 'interaction analysis' which provides a systematic method for understanding passive interactions.

Our wrist control method enables grasping with no internal hand actuation. Using this approach, we show that open-loop control can be used to grasp spheres with changing size up to $\pm 50\%$ from the original training object (figure 14). In addition, we demonstrate how these trajectories, through 'interaction analysis' can be applied in more general cases with grasping everyday objects with significant deviations in size and shape (figure 15). Further development of this type of wrist control may offer some insight into human wrist motions, where proprioception from interactions enable adaptation [30], and motions can potentially be understood as sub-movements to achieve intermediate goals [31].

Many aspects of this work are transferable to other robot hands, and other scenarios or problems. Fundamentally, the interaction analysis approach is transferable for trajectory adaptation for hands incorporating passivity. In addition, interaction-based trajectory adaptation in conjunction with programing by demonstration offers a simple method of generating trajectories capable of reproducing high-level tasks which are robust to geometric changes in the object–environment. Our controller only requires a single input demonstration trajectory and is independent of the design of the hand. Therefore, this approach is readily applicable in other systems, especially those dealing with significant variations in objects or those which require rapid training of new tasks. While this approach can be applied to simple hand–arm systems, the benefits more clearly emerge

when the hand itself has a diverse range of passive behaviours which can be exploited.

In this work, the passive hand provides a test bed for the wrist controller. However, as demonstrated by the range of grasps that can be achieved, the passive hand itself has a number of potential applications, including prosthetics. The hand appears life-like, and the passive properties could assist with everyday grasping and manipulation tasks. The advantages of this hand compared to other prosthetic hands are the low-cost, light-weight and absence of any power source. However, the low holding force from no actuation is a potential limitation.

5.1. Future work

One current limitation of this system is the hand-crafted, manual processes required in the trajectory processing stage, figure 5, requiring an experienced human operator, which limits its applicability. With more processes automated, especially the classification of key states, applicability would greatly increase. Automation of this is potentially achieved through proprioception to measure when and how each finger interact [18, 32, 33], or through visual data. Additionally, humans use proprioceptive and visual feedback to aid in adaptation [30], incorporation of these elements into our system towards more closed-loop control can improve grasping robustness and allow exploration; potentially for learning its own key state update policy.

The trajectory generator can also be applied for learning in-hand manipulation [34]. This is traditionally difficult, generally requiring powerful simulation and learning techniques [35]. By exploiting interactions of passive elements of the hand with the environment, some degree of in-hand manipulation may be possible.

Finally, the passive hand itself can be developed further. The grasping capabilities are limited by the starting posture. Even adding a single actuator (potentially through muscle synergies [19]) could greatly improve the range of tasks that can be completed with our wrist controller, by effectively increasing the number of starting postures in addition to incorporating some internal hand control into completing the task.

Data availability statement

The data that support the findings of this study are available upon reasonable request from the authors.

Acknowledgments

Thanks to the EPSRC Doctoral Training Programme Studentship (RG99055) and Arm Ltd for funding this project.

ORCID iDs

Kieran Gilday https://orcid.org/0000-0002-8264-1535
Josie Hughes https://orcid.org/0000-0001-8410-3565
Fumiya Iida https://orcid.org/0000-0001-9246-7190

References

[1] Ata A A 2007 Optimal trajectory planning of manipulators: a review *J. Eng. Sci. Technol.* **2** 32–54
[2] Bicchi A 2000 Hands for dexterous manipulation and robust grasping: a difficult road toward simplicity *IEEE Trans. Robot. Autom.* **16** 652–62
[3] Toussaint M A, Allen K R, Smith K A and Tenenbaum J B 2018 Differentiable physics and stable modes for tool-use and manipulation planning *2018 Robotics: Science and Systems*
[4] Della Santina C *et al* 2017 Postural hand synergies during environmental constraint exploitation *Front. Neurorob.* **11** 41
[5] Xu Z and Todorov E 2016 Design of a highly biomimetic anthropomorphic robotic hand towards artificial limb regeneration *2016 IEEE Int. Conf. on Robotics and Automation (ICRA)* (IEEE) 3485–92
[6] Kröger T 2010 Literature survey: trajectory generation in and control of robotic systems *On-Line Trajectory Generation in Robotic Systems* (Berlin: Springer) pp 11–31
[7] Eppner C, Deimel R, Álvarez-Ruiz J, Maertens M and Brock O 2015 Exploitation of environmental constraints in human and robotic grasping *Int. J. Robot. Res.* **34** 1021–38
[8] Eppner C and Brock O 2015 Planning grasp strategies that exploit environmental constraints *2015 IEEE Int. Conf. on Robotics and Automation (ICRA)* (IEEE) 4947–52
[9] Amend J R, Brown E, Rodenberg N, Jaeger H M and Lipson H 2012 A positive pressure universal gripper based on the jamming of granular material *IEEE Trans. Robot.* **28** 341–50
[10] Mattar E 2013 A survey of bio-inspired robotics hands implementation: new directions in dexterous manipulation *Robot. Auton. Syst.* **61** 517–44
[11] Deshpande A D, Gialias N and Matsuoka Y 2011 Contributions of intrinsic visco-elastic torques during planar index finger and wrist movements *IEEE Trans. Biomed. Eng.* **59** 586–94
[12] Hughes J A E, Maiolino P and Iida F 2018 An anthropomorphic soft skeleton hand exploiting conditional models for piano playing *Sci. Robot.* **3** eaau3098
[13] Hughes J, Culha U, Giardina F, Guenther F, Rosendo A and Iida F 2016 Soft manipulators and grippers: a review *Front. Robot. AI* **3** 69
[14] Lee M A, Zhu Y, Srinivasan K, Shah P, Savarese S, Fei-Fei L, Garg A and Bohg J 2019 Making sense of vision and touch: self-supervised learning of multimodal representations for contact-rich tasks *2019 Int. Conf. on Robotics and Automation (ICRA)* (IEEE) 8943–50
[15] Hatanaka T, Chopra N and Spong M W 2015 Passivity-based control of robots: historical perspective and contemporary issues *2015 54th IEEE Conf. on Decision and Control (CDC)* 2450–2
[16] Gabellieri C *et al* 2020 Grasp it like a pro: grasp of unknown objects with robotic hands based on skilled human expertise *IEEE Robot. Autom. Lett.* **5** 2808–15
[17] Deimel R and Brock O 2016 A novel type of compliant and underactuated robotic hand for dexterous grasping *Int. J. Robot. Res.* **35** 161–85
[18] Gilday K, George Thuruthel T and Iida F 2020 A vision-based collocated actuation-sensing scheme for a

compliant tendon-driven robotic hand *2020 3rd IEEE Int. Conf. on Soft Robotics (RoboSoft)* (IEEE)
[19] Catalano M G, Grioli G, Farnioli E, Serio A, Bonilla M, Garabini M, Piazza C, Gabiccini M and Bicchi A 2016 From soft to adaptive synergies: the pisa/IIT softH and *Human and Robot Hands: Sensorimotor Synergies to Bridge the Gap between Neuroscience and Robotics* ed M Bianchi and A Moscatelli (Berlin: Springer) pp 101–25
[20] Jones L A and Lederman S J 2006 *Human Hand Function* (Oxford: Oxford University Press)
[21] Feix T, Romero J, Schmiedmayer H-B, Dollar A M and Kragic D 2015 The grasp taxonomy of human grasp types *IEEE Trans. Hum.-Mach. Syst.* **46** 66–77
[22] Grebenstein M, Chalon M, Hirzinger G and Siegwart R 2010 A method for hand kinematics designers 7 billion perfect hands *2010 1st Int. Conf. on Applied Bionics and Biomechanics (ICABB)*
[23] Lazenby R A, Cooper D M L, Angus S and Hallgrímsson B 2008 Articular constraint, handedness, and directional asymmetry in the human second metacarpal *J. Hum. Evol.* **54** 875–85
[24] Krishnan J and Chipchase L 1997 Passive axial rotation of the metacarpophalangeal joint *J. Hand Surg.* **22** 270–3
[25] Çulha U and Iida F 2016 Enhancement of finger motion range with compliant anthropomorphic joint design *Bioinspiration Biomimetics* **11** 026001
[26] Knutson J S, Kilgore K L, Mansour J M and Crago P E 2000 Intrinsic and extrinsic contributions to the passive moment at the metacarpophalangeal joint *J. Biomech.* **33** 1675–81
[27] Pollard N S and Gilbert R C 2002 Tendon arrangement and muscle force requirements for human-like force capabilities in a robotic finger *Proc. 2002 IEEE Int. Conf. on Robotics and Automation (Cat. No. 02CH37292)* vol 4 (IEEE) 3755–62
[28] Wilkinson D D, Weghe M V and Matsuoka Y 2003 An extensor mechanism for an anatomical robotic hand *2003 IEEE Int. Conf. on Robotics and Automation (Cat. No. 03CH37422)* vol 1 (IEEE) 238–43
[29] Chao E Y 1989 *Biomechanics of the Hand: A Basic Research Study* (Singapore: World Scientific)
[30] Scheidt R A, Conditt M A, Secco E L and Mussa-Ivaldi F A 2005 Interaction of visual and proprioceptive feedback during adaptation of human reaching movements *J. Neurophysiol.* **93** 3200–13
[31] Ohta K, Svinin M M, Luo Z, Hosoe S and Laboissiere R 2004 Optimal trajectory formation of constrained human arm reaching movements *Biol. Cybern.* **91** 23–36
[32] Hughes J and Iida F 2017 Localized differential sensing of soft deformable surfaces *2017 IEEE Int. Conf. on Robotics and Automation (ICRA)* (IEEE) 4959–64
[33] Culha U, Wani U, Nurzaman S G, Clemens F and Iida F 2014 Motion pattern discrimination for soft robots with morphologically flexible sensors *2014 IEEE/RSJ Int. Conf. on Intelligent Robots and Systems* (IEEE) 567–72
[34] Dafle N C *et al* 2014 Extrinsic dexterity: in-hand manipulation with external forces *2014 IEEE Int. Conf. on Robotics and Automation (ICRA)* (IEEE) 1578–85
[35] Andrychowicz O M *et al* 2020 Learning dexterous in-hand manipulation *Int. J. Robot. Res.* **39** 3–20